

Characteristics of a Mower Robot with Swing Mower Mechanism by Simulation

Ryota Suzuki¹ and Yoshihisa Uchida²

¹Graduate School of Engineering, Aichi Institute of Technology, Yachigusa 1247, Yakausacho, Toyota 470-0392, Japan

²Aichi Institute of Technology, Yachigusa 1247, Yakausacho, Toyota 470-0392, Japan

Keywords: Mower Robot, Swing Mower Mechanism, Lever-crank Mechanism, Swath, Torque, Velocity, Centroid Movement, Sideslip, Energy Consumption, Operation Time.

Abstract: This study proposes a new mower robot with a swing mower mechanism for advantages such as a string trimmer and a wide swath. The proposed swing mower mechanism is designed for installation in the main body of a four-wheel drive mower robot AMR-D01. The AMR-D01 had overall dimensions as follows: 0.60 m length, 0.50 m width, and 0.30 m height; it weighs 28 kg and maximum velocity is 1.29 m/s. The swing mower mechanism is based on the lever-crank mechanism and translates motor rotation into swing of the rotary blade. We model the mechanism and simulate the characteristics of the centroid movement, sideslip, energy consumption, and operation time to evaluate the swing mower mechanism. The robot velocity is controlled to prevent the occurrence of the unmown spot. Swath is increased from 0.24 m to 0.62 m by 2.58 using the mechanism. The operation time is also decreased by 1/2.58. The swing mower mechanism does not have much influence on the robot movement. The change of the static friction coefficient and the slope angle also does not have much influence on the sideslip of the robot under the present conditions. The energy consumption increases with the increasing robot velocity.

1 INTRODUCTION

A string trimmer is light and small and can easily treat; therefore, the trimer is widely used. However, it requires heavy work, takes time to work, and have a serious safety issue (Hanidza, 2013). Thus, the string trimer automation is needed to overcome these problems. Various string trimmer robots, such as handle-, passenger-, and remote-type robots, are used until now.

HAMMER KNIFE (OREC, 2018) and HR663 (YAMABIKO, 2018) are commercialized as the handle type. These trimmers are very convenient, but the user must control behind the machine. Ride on Brush Cutter “RABBIT” (OREC, 2018), RMJ800 (YAMABIKO, 2018), ZHM1520 (ZENOAH, 2018), and Mid-mower (Jun, 2008) are commercialized and proposed as passenger type. These are very useful for large area, but user must ride and drive the machine and machine is heavy weight. Miimo (Honda, 2018) and HUSQVARNA AUTOMOWER® 315 (Husqvarna, 2018) are commercialized and proposed as the remote type. These trimmers are small and safe, but are mainly for the lawn.

Challenges for practical application of mower robot are obstacle detection and avoidance, miniaturization for efficiency and optimization, path planning and tacking, ability to move on rough terrain, and efficiency of grass cutting. Several researchers have proposed to overcome these problems.

Most mower robots are intended to operate on agricultural land, garden, rice field and river bed. However, such areas are not free from interactions with humans, whose safety and legal positions must be considered. Christiansen et.al. (Christiansen, 2017) proposed a sensor platform in autonomous mowing operation to detect a human using several cameras. This platform is for a tractor, thus, the entire platform is large. In contract, small robots for agriculture are paying attention for efficiency and optimization (Basu, 2018). Path planning methods for agriculture robot are proposed (Urrea, 2015, Wang, 2014, Ohkawa, 2014, Hameed, 2014). These methods are useful for mower robot. Improvement of movement performance and efficiency of grass cutting on small robot are remaining issues.

We develop remote-controlled mower robots in our laboratory. The developed mower robot is usable even on a slope ground. However, they have

disadvantages, such as small swath and long operation time. In addition, grass, which is not mowed, hit against the front body of the robot because its blade diameter is smaller than the width of the robot body. This study develops a new mower robot, which has the goal to reach convenience like a string trimmer, has a wide swath, and an autonomous travel.

This study proposes a new mower robot with a swing mower mechanism for convenience like a string trimmer and a wide swath. Three methods, namely multiple-blade, large-blade, and swing-blade methods, are used to acquire a wide swath. The multiple-blade method can have an unmown spot in-between blades. The large blade needs a high cutting energy. Although the mechanism of the swing-blade method is complex, it can use an existing blade. Thus, we selected the swing-blade method by the swing mower mechanism. We discuss the centroid movement for static characteristics, sideslip for dynamic characteristics, energy consumption, and operation time.

2 MOWER ROBOT

The proposed swing mower mechanism was designed for installation in the main body of the four-wheel drive mower robot, AMR-D01. The robot had main dimensions of 0.60 m length, 0.50 m overall width, and 0.30 m overall height. It had a total weight of 28 kg and a maximum velocity of 1.29 m/s (Figure 1).

AMR-D01 consisted of a blade for cutting and the main body. The blade was attached to the front of the main body. The control system of the robot consisted of a control circuit, a drive circuit, motors for drive, blade and swing, and sensors. The robot received the control signal from the remote controller. The robot then properly moved using feedback control.

The swing mower mechanism was based on the lever-crank mechanism and translated motor rotation into swing of the rotary blade (Figure 2). The rotation of link AB was translated into the swing of link CD with joint D as a supporting point using the drive motor for this mechanism installed at joint A. In this mechanism, the r_b radius rotary blade installed at joint C swings from side to side. The counter clockwise angles of links AB and CD with datum line AD are θ and φ , respectively. For the symmetric swing, the mechanism was rotated by β .

The AMR-D01 parameters are as follows: mass of the robot main body $m_r = 26.4$ kg; mass of the blade $m_b = 1.6$ kg; mass of the swing mower mechanism $m_s = 0$ kg; radius of the wheel $r_t = 0.1$ m; radius of the

blade $r_b = 0.12$ m; and lengths of the link $a = 0.060$ m, $b = 0.430$ m, $c = 0.382$ m, and $d = 0.139$ m. In this case, the angle β is 0.25 rad from the calculation. The x and y axes are set as shown in Figure 2. The origin O is at the center of the robot body.



Figure 1: Photograph of the mower robot AMR-D01.

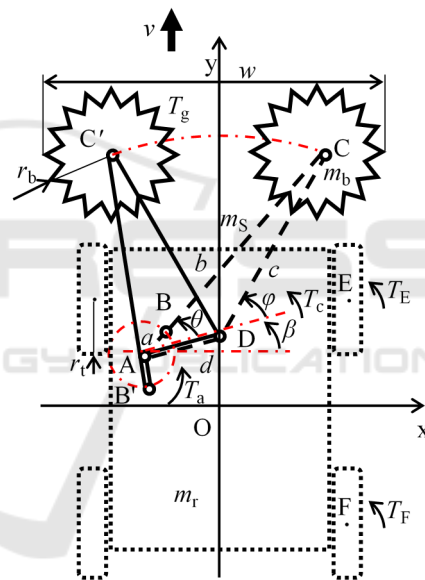


Figure 2: Schematics of the mowing robot.

3 SIMULATION

We modeled the mechanism and simulated the characteristics of the centroid movement, sideslip, energy consumption, and operation time to evaluate the swing mower mechanism.

The angular velocity of link AB, $\dot{\theta}$, is given as follows to prevent the unmown spot occurrence:

$$\dot{\theta} = \frac{\pi v}{r_b} \tag{1}$$

where, v is the robot velocity.

The swath w by swing is obtained as follows:

$$w=2r_b+c\sqrt{2\{1-\cos(\varphi_{\max}-\varphi_{\min})\}} \quad (2)$$

where, φ_{\max} and φ_{\min} are the maximum and minimum of φ , respectively.

Considering the moment of inertia and the load torque from grass T_g , torque T_c that occurs in link CD by the swing blade is given as Eq. (3).

$$T_c=m_b\ddot{\varphi}\left(\frac{1}{2}r_b^2+c^2\right)+T_g \quad (3)$$

The torque required link, AB, T_a is obtained as follows using the angular velocity ratio of links AB and CD:

$$T_a=\frac{\dot{\varphi}}{\dot{\theta}}T_c \quad (4)$$

The required torque of the swing motor is calculated using Eq. (4).

We evaluate the centroid movement for the static characteristics. Assuming that the mass of the swing mower mechanism is negligible, $m_s=0$, because this mass is much smaller than the mass of the body. The centroid of the robot $G(G_x, G_y)$ is calculated from the following equations:

$$G_x=\frac{m_bcc\cos(\varphi+\beta)}{m_r+m_b} \quad (5)$$

$$G_y=\frac{m_b\{c\sin(\varphi+\beta)+y_1\}}{m_r+m_b} \quad (6)$$

Figure 3 shows the centroid movement in a period of swing. The results show that the centroid movement is small against the robot size. Thus, the swing mower mechanism does not have much influence on the robot movement.

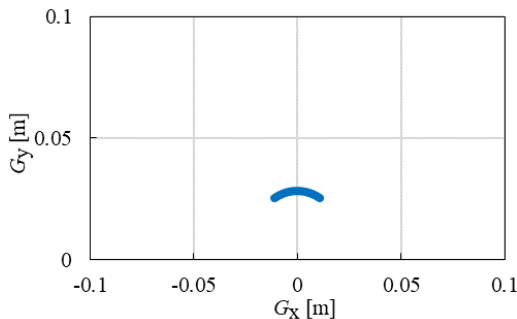


Figure 3: Characteristic of the centroid movement of the robot.

We discuss herein the sideslip for the dynamic characteristics. The torque around joint D at the front and rear tires (i.e., T_E and T_F , respectively) are expressed as follows:

$$T_E=\mu_0Nq_1 \quad (7)$$

$$T_F=\mu_0Nq_2 \quad (8)$$

where, μ_0 is the static friction coefficient; N is the normal reaction; q_1 is the distance between joint D (0, y_1) and the contact point of the front tire, E (x_1, y_2); q_2 is the distance between joint D (0, y_1) and the contact point of the rear tire, F (x_1, y_3). The centroid movement is small against the robot size; hence, the normal reaction N is given by Eq. (9) as follows:

$$N=\frac{1}{4}(m_r+m_b)g\cos\alpha \quad (9)$$

where, α is the slope angle, and g is the gravity acceleration. Using the Pythagorean theorem, the distances of q_1 and q_2 are given as follows:

$$q_1=\sqrt{x_1^2+(y_2-y_1)^2} \quad (10)$$

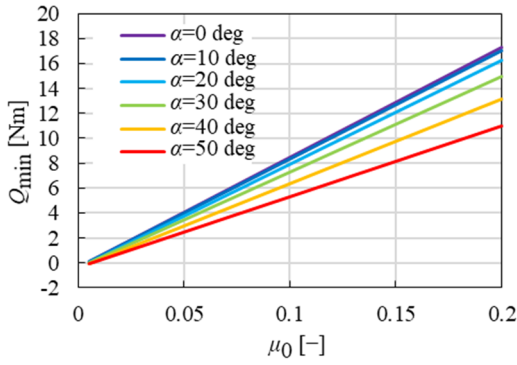
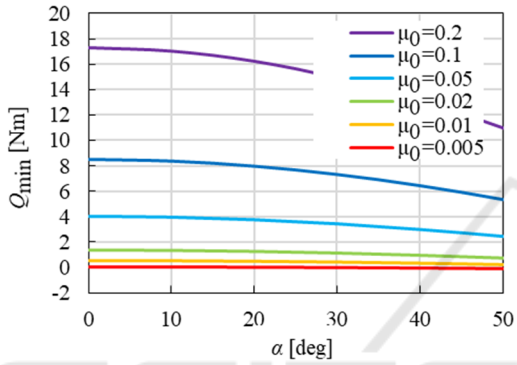
$$q_2=\sqrt{x_1^2+(y_1-y_3)^2} \quad (11)$$

The sideslip does not occur when the sum of the torque at each tire is larger than torque T_c . For simplicity, variable Q is defined as follows:

$$Q=2(T_E+T_F)-T_c \quad (12)$$

The sideslip of the robot does not occur when Q is positive. Figure 4 shows the minimum value of Q during one period as a function of the static friction coefficient for various slope angles α . Variable Q_{\min} increases with the increasing friction coefficient for all slope angle conditions. Figure 5 presents variable Q_{\min} as a function of the slope angle. Variable Q_{\min} decreases with the increasing slope angle. Variable Q_{\min} is a negative value when μ_0 is smaller than 0.05.

These results indicate that the change of μ_0 and α does not have much influence on the sideslip of the robot under actual possible use conditions.


 Figure 4: Q_{\min} as a function of the static friction coefficient.

 Figure 5: Q_{\min} as a function of the slope angle.

The proposed method has the swing mower mechanism that needs additional energy. Therefore, we perform a comparison of the characteristics with and without the swing mower mechanism to evaluate the robot's energy consumption.

The energy consumption of the existing mower robot, P_A , is expressed with the energy consumption of the drive motor for moving, P_{At} and the blade motor for the rotary blade, P_{Ab} .

$$P_A = P_{At} + P_{Ab} \quad (13)$$

In the same manner, the energy consumption of the robot with the swing mower mechanism, P_S , is expressed as follows with the energy consumption of the drive motor, P_{St} , blade motor, P_{Sb} , and swing motor for the swing mower mechanism, P_{Ss} :

$$P_S = P_{St} + P_{Sb} + P_{Ss} \quad (14)$$

The energy consumption of each drive motor, P_{At} and P_{St} , is expressed as follows:

$$P_{At} = \left(\frac{\pi}{30} n_{At} T_{At} + \frac{K_{t_n/T} T_{At}^2}{K_{t_T} K_{t_n}} \right) t_A \quad (15)$$

$$P_{St} = \left(\frac{\pi}{30} n_{St} T_{St} + \frac{K_{t_n/T} T_{St}^2}{K_{t_T} K_{t_n}} \right) t_S \quad (16)$$

where, $K_{t_n/T}$ is the rotation number–torque gradient; K_{t_T} is the torque constant; K_{t_n} is the rotation number constant; n_{At} and n_{St} are the rotation numbers of each drive motor; T_{At} and T_{St} are the torques of each drive motor; and t_A and t_S are the operation times of the robot. n_{At} and n_{St} are given as Eq. (17),

$$n_{At} = n_{St} = \frac{30 v i_t}{\pi r_t} \quad (17)$$

where, i_t is the speed reduction ratio of the gear head. T_{At} and T_{St} are given as Eqs. (18) and (19), respectively,

$$T_{At} = \frac{m_r + m_b}{i_t \eta_t} (\sin \alpha + \mu \cos \alpha) g r_t \quad (18)$$

$$T_{St} = \frac{m_r + m_b + m_s}{i_t \eta_t} (\sin \alpha + \mu \cos \alpha) g r_t \quad (19)$$

where, μ is the dynamic friction coefficient, and η_t is the transmission efficiency.

The energy consumptions of the blade motor, P_{Ab} and P_{Sb} , are expressed as follows:

$$P_{Ab} = \left(\frac{\pi}{30} n_b K_{b_T} I_b + \frac{K_{b_T} K_{b_n/T} I_b^2}{K_{b_n}} \right) t_A \quad (20)$$

$$P_{Sb} = \left(\frac{\pi}{30} n_b K_{b_T} I_b + \frac{K_{b_T} K_{b_n/T} I_b^2}{K_{b_n}} \right) t_S \quad (21)$$

where, $K_{b_n/T}$ is the rotation number–torque gradient; K_{b_T} is the torque constant; K_{b_n} is the rotation number constant; n_b is the rotation number of the blade motor; and I_b is the motor current.

The energy consumption of the swing motor, P_{Ss} , is expressed as follows:

$$P_{Ss} = I_S V_S t_S \quad (22)$$

where, I_S is the swing motor current, and V_S is the input voltage.

The rotation number n_{Ss} and the torque T_{Ss} of the swing motor are expressed as follows:

$$n_{Ss} = \frac{30 \dot{\theta}_S}{\pi} \quad (23)$$

$$T_{Ss} = \frac{1}{i_S \eta_S} T_a \quad (24)$$

where, i_s is the speed reduction ratio of the gear head, and η_s is the transmission efficiency of the swing motor. I_s is calculated using these equations and the motor specifications.

The simulation conditions are as follows:
 $n_b = 5631 \text{ rpm}$, $I_b = 1.35 \text{ A}$, $V_s = 24 \text{ V}$,
 $K_{m/T} = 8.69 \times 10^3 \text{ rpm/Nm}$, $K_{t/T} = 25.9 \times 10^{-3} \text{ Nm/A}$,
 $K_{t_n} = 369 \text{ rpm/V}$, $K_{b_n/T} = 20.6 \times 10^3 \text{ rpm/Nm}$,
 $K_{b_T} = 24.3 \times 10^{-3} \text{ Nm/A}$, and $K_{b_n} = 393 \text{ rpm/V}$.

Figure 6 shows the typical results of the energy consumption per square meter at the conditions of $\alpha = 0$ and $\mu = 0.3$. A comparison with and without the swing mower mechanism shows that the energy consumption with the swing mower mechanism is larger than the energy consumption without the swing mower mechanism.

Figure 7 shows the characteristics of the operation time per square meter with and without the swing mower mechanism. Using the mechanism, the swath is increased from 0.24 m to 0.62 m by 2.58. Therefore, the operation time per square meter is also decreased by 1/2.58 under the condition of the same robot velocity. The swing mower mechanism effectively increases the swath and decreases the operation time.

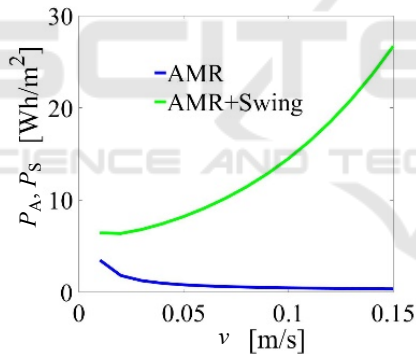


Figure 6: Results of the energy consumption.

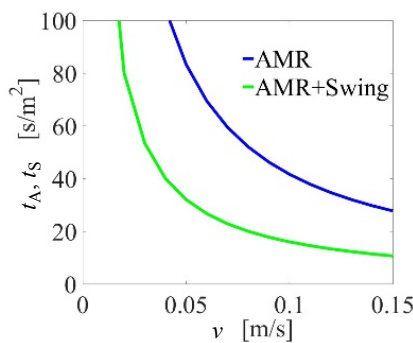


Figure 7: Results of the operation time.

4 CONCLUSIONS

We proposed the swing mower mechanism for a mower robot. We modeled the mechanism and simulated the characteristics of the centroid movement, sideslip, energy consumption, and operation time to evaluate the swing mower mechanism.

The findings obtained are as follows:

- 1) The robot velocity and the angular velocity of link AB were controlled to prevent the unmown spot occurrence.
- 2) The centroid movement was small against the robot size. Thus, the centroid movement did not have much influence on the robot movement.
- 3) We also discussed the sideslip for the dynamic characteristics. The change of the static friction coefficient and the slope angle also did not have much influence on the sideslip of the robot under the present conditions.
- 4) We performed a comparison of the characteristics with and without the swing mower mechanism to evaluate the energy consumption of the robot. The energy consumption with the swing mower mechanism was larger than the energy consumption without the swing mower mechanism.
- 5) The swath was increased from 0.24 m to 0.62 m by 2.58. Therefore, the operation time per square meter was also decreased by 1/2.58. The swing mower mechanism effectively increased the swath and decreased the operation time.

For the future work, we will build the mower robot and experimentally evaluate the robot. For the autonomous travel, we will construct a self-location estimation system running with Kalman filter using GNSS and inertial sensors. Moreover, the load torque will be applied to control the blade motor by the robot velocity related to a change in the amount of grass.

ACKNOWLEDGEMENTS

This work was partially supported by JSPS KAKENHI Grant Number JP17K06279 and a special research grant from Aichi Institute of Technology, Japan.

REFERENCES

- Hanidza, T., Jan, A., Abdullah, R., Ariff, M., 2013. *Procedia, Social and Behavioral Sci.*, Vol. 90, pp. 661–672.
- OREC, 2018. <http://www.orec-jp.com/en/products.html>.
- YAMABIKO, 2018. <http://www.yamabiko-corp.co.jp/kioritz/products/category/detail/id=9549>.
- YAMABIKO, 2018. <http://www.yamabiko-corp.co.jp/kioritz/products/category/detail/id=2108>.
- ZENOAH, 2018. <http://www.zenoah.co.jp/int/products/flail-mowers/zhm1520/>.
- Jun, H., Choi, Y., Lee, C., Kang, Y., 2008. *Engineering in Agriculture, Environment and Food* Vol. 1, No. 1, pp. 39–44.
- Honda, 2018. <http://world.honda.com/powerproducts-technology/miimo/>.
- Husqvarna, 2018. <http://www.husqvarna.com/us/products/robotic-lawn-mowers/automower-315/967623405/>.
- Christiansen, P., Kragh, M., Steen, K. A., Karstoft, H., Jørgensen, R. N., 2017. *Precision Agriculture*, Volume 18, Issue 3, pp. 350–365.
- Basu, S., Omotubora, A., Beeson, M., Fox, C., 2018. *AI & SOCIETY*, pp. 1-22.
- Urrea, C., Muñoz, J., 2015. *Journal of Intelligent & Robotic Systems*, Volume 80, Issue 2, pp. 193–205.
- Wang, P., Meng, Z., Luo, C., Mei, H., 2013. *Computer and Computing Technologies in Agriculture VII*, pp. 242–248.
- Ohkawa, S., Takita, Y., Date, H., 2014. *Transactions of the JSME*, Vol. 80, No. 812 (in Japanese).
- Hameed, I. A., 2014. *Journal of Intelligent & Robotic Systems*, Volume 74, Issue 3–4, pp. 965–983.